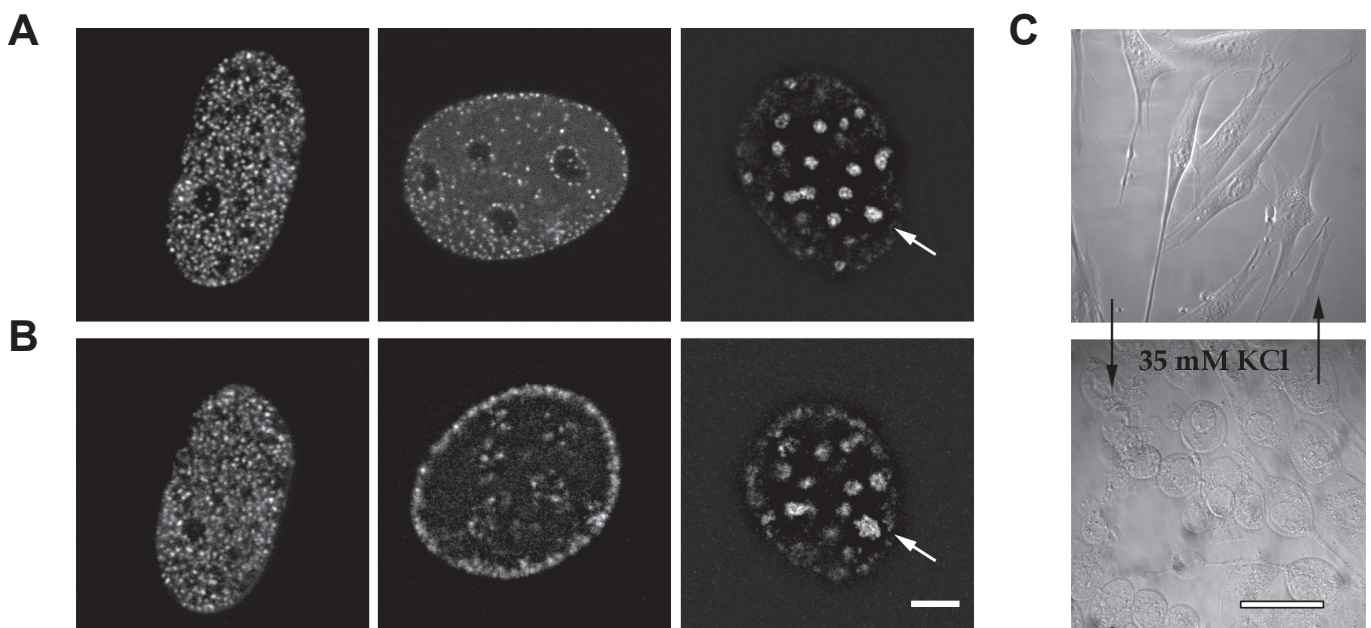


**Table S1: Summary of SMI measurements from all three labelling techniques**

Statistical testing was performed using the Kolmogorov-Smirnov test and the corresponding p-values are shown. Green colouring indicates that the null hypothesis that the distributions are equal can be rejected on a 95% confidence interval and red colouring that it is not possible to reject the null hypothesis. Due to the very large sample size, the small differences present in the BrdU labelling were all statistically significant. The GFP labelling showed somewhat larger differences, which were also significant when comparing the early with the mid and/or late distributions. It however suffered a little from the small sample size in terms of late foci.

		Parameters				KS Test p-value	
		Mean [nm]	s.d. [nm]	# foci	# cells	Mid	Late
BrdU	Early	123.5	32.2	17572	29	5e-26	3e-38
	Mid	127.1	31.5	13041	24		0.0062
	Late	128.6	31.1	10897	18		
GFP-PCNA	Early	109.9	39.1	252	6	7e-6	0.0013
	Mid	128.8	40.2	399	14		0.1576
	Late	138.3	39.3	24	2		
abGFP-PCNA	Early	99.0	40.1	972	14	0.0117	0.2381
	Mid	106.2	40.6	269	6		0.0415
	Late	98.0	34.5	154	6		



### Figure S1

Changes of the RF patterns after in vivo hypotonic treatment

(A) The three main patterns of replication foci (RF) that appear in course of S-phase are presented. From left to right: early, middle and late S-phase. Representative confocal optical sections of RF in untreated live GFP-PCNA expressing mouse cells as in Fig. 1.

(B) The same patterns after 5 min in vivo hypotonic treatment. Culture medium was removed from the cells at the microscope stage and pre-warmed 35 mM KCl solution was added to the LabTech TM microscopy chamber (See also Materials and Methods). Late S-phase pattern is composed of apparently more complex RF and drastic changes were visible with late S-phase RF, whose substructures became discernible (see arrow). Scale bar 5  $\mu\text{m}$ .

(C) Effect of hypotonic treatment on the shape of live cells is shown in the phase contrast images. Scale bar 50  $\mu\text{m}$ .

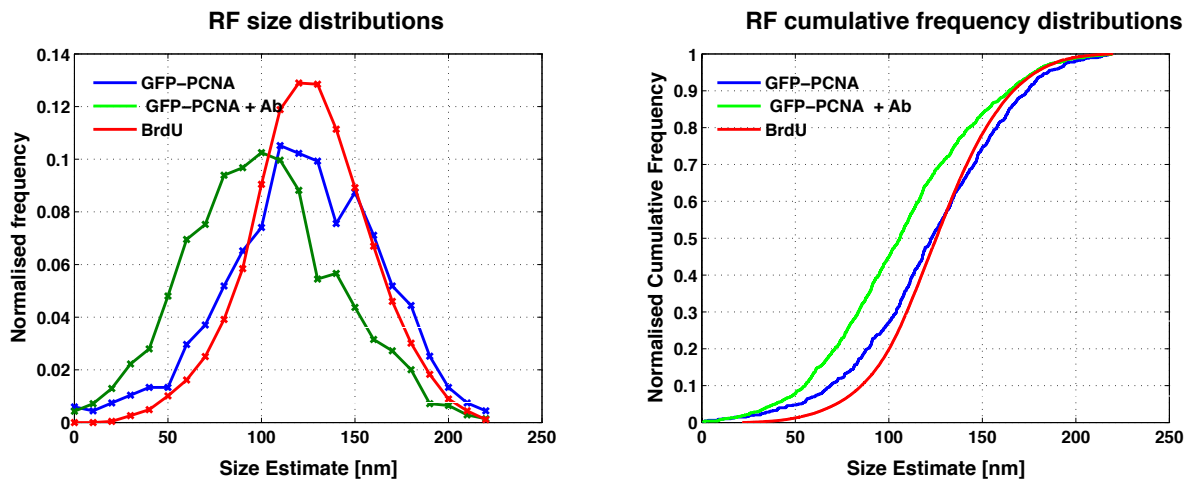


**Figure S2**

Comparison of RF size distribution from the different labeling methods

The different labeling techniques resulted in size distributions, which, while not hugely different, showed larger differences than those observed between the S-phase stages within one labeling method. The comparison between the labeling techniques is shown here based on all the cells from each method irrespective on S-phase stage.

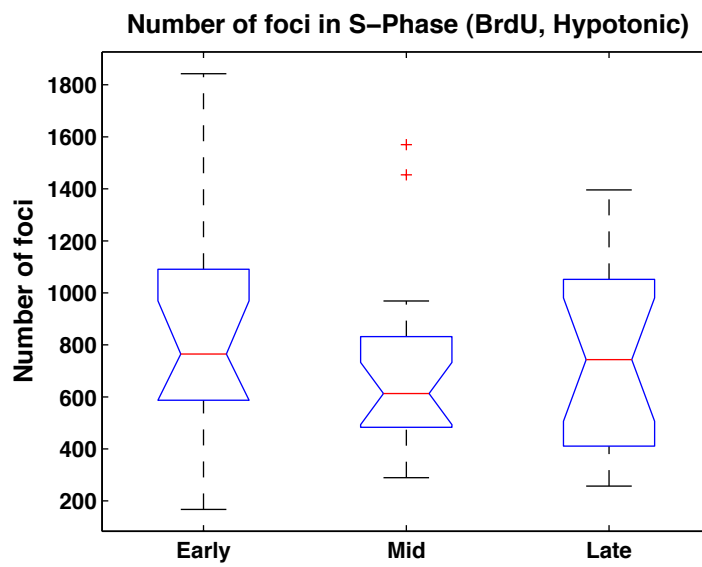


**Figure S3**

Variability of RF numbers measured with SMI microscopy

Number of foci present at different stages in the S-phase estimated from the hypotonic, whole cell, preparations. Our results showed a high variability in the number of foci detected throughout the S-phase, with both the largest number and also the largest variation present in the early S-phase.

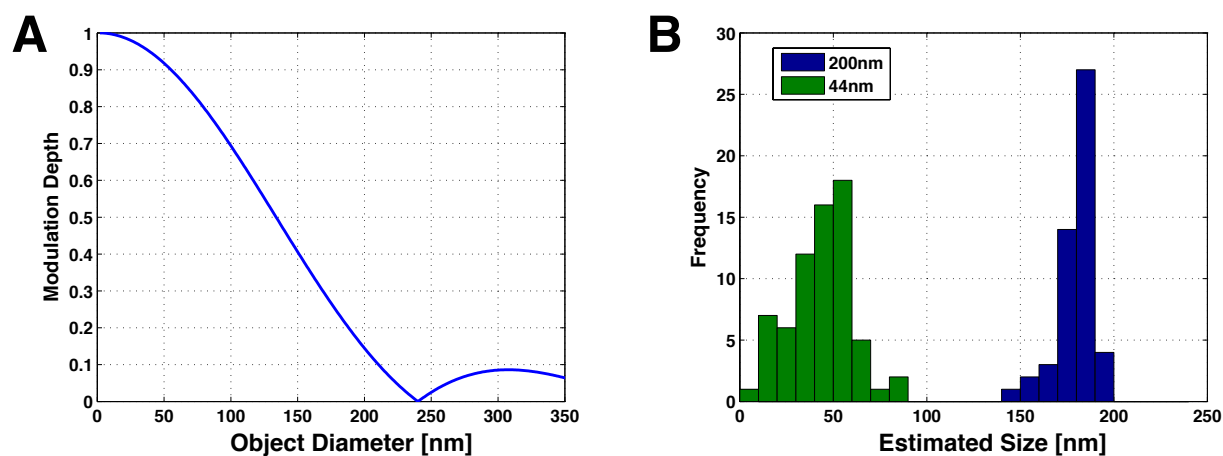


**Figure S4**

Calibration of the SMI setup

(A) Curve relating the depth of modulation retained in SMI image to object size for a spherical object model and an excitation wavelength of 488nm and immersion in glycerol ( $n=1.46$ ).

(B) Measured size distributions of 44 nm (left) and 200 nm (right) fluorescent beads used as calibration objects for SMI microscopy. Note that the broad distribution obtained from the 44 nm beads relates to the poor photon statistics obtainable from this sample.